MARTIN MARIETTA ENERGY SYSTEMS LIBRARIES

3 4456 0315283 4

ORNL/TM-11562

ornl

OAK RIDGE
NATIONAL
LABORATORY

MARTIN MARIETTA

Model for Particle Balance in Pumped Divertors (pre-VORTEX)

J. T. Hogan

OAK RIDGE NATIONAL LABORATORY
CENTRAL RESEARCH LIBRARY
CIRCULATION SECTION
4500N ROOM 175
LIBRARY LOAN COPY
DO NOT TRANSFER TO ANOTHER PERSON
If you wish someone else to see this report, send in name with report and the library will arrange a loan.

OPERATED BY
MARTIN MARIETTA ENERGY SYSTEMS, INC.
FOR THE UNITED STATES
DEPARTMENT OF ENERGY

This report has been reproduced directly from the best available copy.

Available to DOE and DOE contractors from the Office of Scientific and Technical Information, P.O. Box 62, Oak Ridge, TN 37831; prices available from (615) 576-8401, FTS 626-8401.

Available to the public from the National Technical Information Service, U.S. Department of Commerce, 5285 Port Royal Rd., Springfield, VA 22161.
NTIS price codes—Printed Copy: A03 Microfiche A01

This report was prepared as an account of work sponsored by an agency of the United States Government. Neither the United States Government nor any agency thereof, nor any of their employees, makes any warranty, express or implied, or assumes any legal liability or responsibility for the accuracy, completeness, or usefulness of any information, apparatus, product, or process disclosed, or represents that its use would not infringe privately owned rights. Reference herein to any specific commercial product, process, or service by trade name, trademark, manufacturer, or otherwise, does not necessarily constitute or imply its endorsement, recommendation, or favoring by the United States Government or any agency thereof. The views and opinions of authors expressed herein do not necessarily state or reflect those of the United States Government or any agency thereof.

ORNL/TM-11562
Dist. Category UC-427

Fusion Energy Division

MODEL FOR PARTICLE BALANCE IN PUMPED DIVERTORS (pre-VORTEX)

J. T. Hogan

Date Published: August 1990

Prepared for the
Office of Fusion Energy
Budget Activity No. AT 05

Prepared by the
OAK RIDGE NATIONAL LABORATORY
Oak Ridge, Tennessee 37831-6285
operated by
MARTIN MARIETTA ENERGY SYSTEMS, INC.
for the
U.S. DEPARTMENT OF ENERGY
under contract DE-AC05-84OR21400

MARTIN MARIETTA ENERGY SYSTEMS LIBRARIES

3 4456 0315283 4

CONTENTS

ABSTRACT v
1. INTRODUCTION 1
2. MODEL 3
   2.1 DIVERTOR CHANNEL 3
   2.2 SCRAPE-OFF LAYER 6
   2.3 PLASMA CORE 7
   2.4 NEUTRAL BALANCE 8
3. RESULTS 9
REFERENCES 15

ABSTRACT

An internally consistent model for particle transport in an open divertor geometry has been developed. Embodied in a new code, pre-VORTEX, the model couples the particle balance in the plasma core, the scrape-off layer, the open divertor channels, and the "vacuum" regions. This mutual coupling is particularly important in determining the conditions required for high recycling in the divertor. The plasma core is considered to have a relatively quiescent core region and a less well confined "edge-localized mode" (ELM) region. The scrape-off layer is modeled with one-dimensional parallel and prependicular transport. A two-point divertor channel model is used; it is similar to previous models, but with the addition of new physical processes: hydrogen charge exchange, impurity thermal charge exchange, and flux-limited parallel transport. Wall recycling data are required to describe the differing recycling properties of the wall regions and the divertor plates. Given local plasma diffusivities and wall recycling properties, the model predicts the volume-averaged density and global particle confinement time. The input data are uncertain, and a major use for the model is to permit comparison with data. The final model, VORTEX, is intended for application to the analysis of divertor confinement experiments; it is coupled to a one-and-one-half–dimensional transport code and uses detailed geometric input from equilibrium fitting codes, experimentally measured core profiles, and such parameters as can be measured in the scrape-off layer. The pre-VORTEX model is compared as a stand-alone code with typical data from the DIII-D experiment and applied to the proposed DIII-D Advanced Divertor Project.

1. INTRODUCTION

The divertor has been the object of study for some time. As described by the ASDEX group, the divertor creates a localized recycling vortex, in which a large particle flux (typically an order of magnitude greater than that of the core plasma efflux) is established at the divertor plate.[1] The conditions for maintaining this high-recycling state are critical for the design of a practical divertor in future devices.[2]

Quantitative analysis of particle confinement in open divertors requires the establishment of a self-consistent, empirically based model for recycling processes. Unlike the previously analyzed case of closed divertors, the typical single-null open divertor allows the exchange of particle flux from one divertor channel directly to the other through the "private flux" region. There are many additional pathways for particle flows, and they are strongly coupled during the typical pulse length (1–30 s) of present tokamaks. (See Fig. 1.) In addition, schemes such as that envisaged for the DIII-D Advanced Divertor Project[3] seek to control the density through active pumping at the outer divertor (region 7 in Fig. 1). Analysis of such effects requires a self-consistent model for the global particle flows.

The model described here incorporates a global description of the particle balance in a single-null open divertor and is intended to complement detailed modeling of neutrals using three-dimensional Monte Carlo codes and two-dimensional plasma scrape-off layer modeling. While the latter incorporate a high degree of geometric realism, the plasma codes are still under development, and coupling of the multidimensional codes is required to make a self-consistent model. This has rarely been done in the past, primarily because of the computational resources required. Also, significant changes are observed in the plasma particle balance that correspond to changes in the wall conditioning method, and detailed models are not required for this problem.

This report describes the pre-VORTEX code, in which the models for the scrape-off layer, divertor channels, and wall recycling are coupled to a simplified plasma model. This development has been carried out as a precursor to the creation of a model in which the plasma is treated with a one-and-one-half–dimensional code, with a detailed description of geometry, plasma core transport, heating, and impurity efects.

Pre-VORTEX treats the parallel mass, momentum, and energy transport for the divertor channels. The scrape-off layer is treated with one-dimensional radial and parallel diffusivities. Neutral gas balance is calculated for the various regions accessible

ORNL-DWG 90-2657 FED

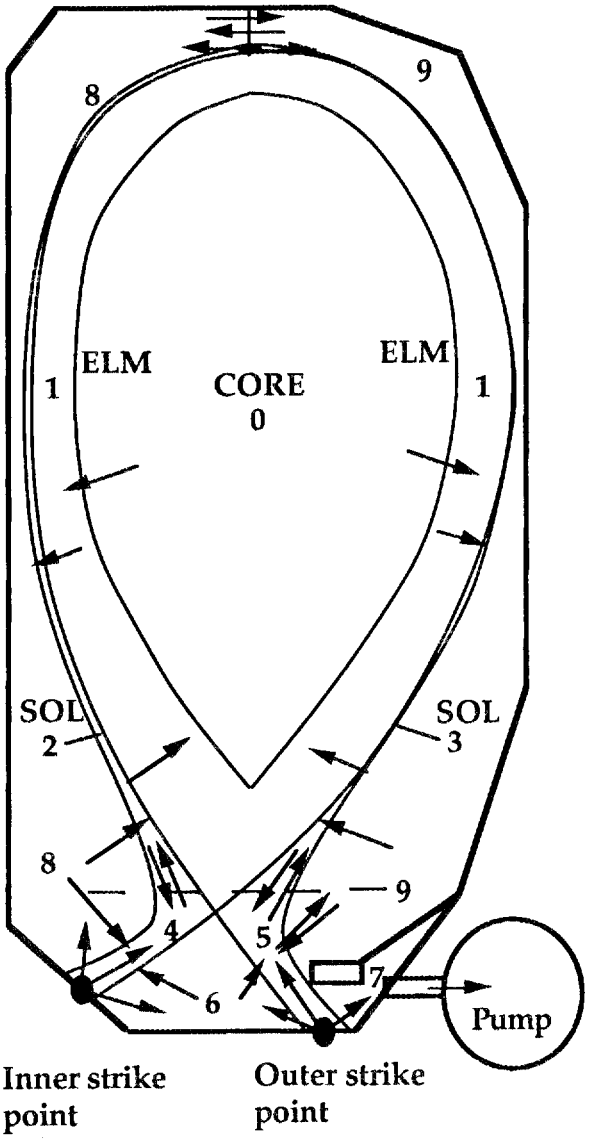

Region	Description
0	Plasma core
1	ELM region
2	Inboard SOL
3	Outboard SOL
4	Inner Divertor Channel
5	Outer Divertor Channel
6	Divertor Recycle
7	Baffle Chamber
8	Inner Plenum
9	Outer Plenum

Fig. 1. Schematic view of regions described in the VORTEX code (DIII-D global divertor model).

for neutrals inside the vessel, and exchange with the wall is treated. The core plasma is divided into a central region and an edge-localized mode (ELM) region, and the particle efflux is expressed in terms of the conventional diffusivity and the ELM frequency and amplitude. Section 2 describes the semi-analytical model, and Sect. 3 presents results.

2. MODEL

The most important requirement for the model is to delineate the conditions required for the establishment of a low-temperature, high-density, high-recycling divertor. Thus, the divertor channel model is described in Sect. 2.1. Then we describe the scrape-off layer equations, which couple the inner and outer channels of the divertor, and the plasma equations for both the core and the ELM region and the wall model.

2.1 DIVERTOR CHANNEL

The divertor channel model is based on earlier work on simplified divertor models.[4] The mass balance equation for the inner divertor channel (region 4 in Fig. 1) is the simplest, since there is no external pump to be applied to this segment. The axial particle balance is as follows:

mass,

$$\frac{1}{b(l)}\frac{\partial}{\partial l}[b(l)nv] = S_0 + \Sigma_{\text{plasma}} \ ;$$

momentum,

$$\frac{1}{b(l)}\frac{\partial}{\partial l}\left[b(l)n\left(v^2 + v_s^2\right)\right] = -\frac{nv}{\tau_{\text{cx}}};$$

energy,

$$-\frac{1}{b(l)}\frac{\partial}{\partial l}\left[b(l)K_0T^{5/2}\frac{\partial T}{\partial l}\right] = -\alpha S_0 - \frac{nT}{\tau_\alpha}.$$

Here n, T, and v are the plasma density, temperature, and parallel flow speed; S_0 is the production rate of cold ions; Σ_{plasma} is the efflux from the plasma into the scrape-off layer; α is the energy loss per ion-electron pair created (which can be enhanced to model

low-Z impurity radiation); and τ_{cx} is the charge-exchange lifetime. The flux tube is assumed to have a width $b(l)$, taken from magnetic analysis. The poloidal sound speed is

$$v_s^2 \equiv \frac{B_{\rm pol}^2}{B_T^2}\sqrt{\frac{2kT}{M}} .$$

The global model requires the net fluxes; thus, integrating from the divertor throat to the plate,

$$\Phi_{\rm plate} = \Phi_{\rm throat} + \frac{F_{\rm plate}(1-\delta)}{\lambda_{\parallel}} \int_{\rm throat}^{\rm plate} dl \;\; b(l)\exp\left(\frac{l-L}{\lambda}\right)$$
$$+\frac{1}{4}\sum_{i=1}^{N}\Gamma_i\left(L_{\perp}^i/L\right)\left[1-\int_{\rm throat}^{\rm plate} dl \;\; \exp\frac{-b(l)}{\lambda_{\perp}}\right] ,$$

where Γ_i is the neutral influx for the channel region from adjacent zones (6 and 8, for the inner channel), $L_{\perp}$ is the poloidal extent of the area through which neutrals enter the divertor channel (which has poloidal length L), N is the total number of regions that contribute a neutral flux to this divertor channel, $\Phi_{\rm plate}$ and $\Phi_{\rm throat}$ are the particle fluxes (particles per unit area per second) at the divertor plate and throat, and δ is the fraction of ions striking the plate that escape from the reflux stream, either through absorption into the divertor plate, escape to the pump, or transit to regions 6 or 8 in Fig. 1. This fraction is expressed, for channel 4, as

$$\delta_4 = (1-R_4)\left\{1-(\eta_{46}+\eta_{48})\left[\exp(-b_4/\Lambda_4)\right]\left[1-\exp(-L_4/\lambda_4)\right]\right\} ,$$

where R_4 is the reflection probability and η_{46} and η_{48} are the probabilities of escape into the central vacuum area (6) and the inner vacuum area (8), respectively.

The corresponding quantity for the outer divertor channel is

$$\delta_5 = (1-R_5)\left\{1-(\eta_{56}+\eta_{59}+\eta_{57})\left[\exp(-b_5/\Lambda_5)\right]\left[1-\exp(-L_5/\lambda_5)\right]\right\} .$$

The perpendicular (Λ) and parallel (λ) mean free paths for ionization are computed from the plate and throat temperatures and densities,

$$\Lambda = \frac{v_{\rm th,plate}}{n_{\rm plate}\langle\sigma v\rangle_{\rm ion,plate}} , \quad \lambda = \frac{v_{\rm th,plate}}{n_{\rm plate}\langle\sigma v\rangle_{\rm ion,throat}} .$$

Integration of these equations leads to solutions for the plate and throat temperatures and densities required for a steady state.

The flux amplification factor is

$$A = \frac{1}{D}\left\{1 + \frac{G}{\Phi_{\text{throat}}}\left[1 - \frac{\Lambda}{\delta b}\exp\left(-\{\delta\} b/\Lambda\right)\right]\right\} ,$$

where

$$D = 1 - (1-\delta)\left[1 - \varepsilon\ \exp(-L/\lambda) - (1-\varepsilon)\frac{\lambda}{L}\left(1 - \exp\frac{-L}{\lambda}\right)\right]$$

and

$$G = 2\pi R L \sum_{i=1}^{N}\left(\frac{\Gamma_I^P}{4}\right)\left(\frac{L_I^P}{L}\right) .$$

The expression for the plate temperature is

$$T_{\text{plate}} = \frac{Q_{\text{throat}}}{\gamma A \Phi_{\text{throat}}} - \frac{\alpha}{\gamma}\frac{A-1}{A} ,$$

where Q_{throat} is the power per unit area entering the throat, γ is the secondary electron emission coefficient, R is the average major radius for this divertor channel, and δb is the variation of the divertor channel width. In this pre-VORTEX model, the channel width is taken as $b(l) = b_{\text{throat}} + \delta b(l - l_{\text{throat}})/L$. The throat temperature is

$$T_{\text{throat}} = \left\{\frac{T_{\text{plate}}^{7/2}}{\varepsilon} + \frac{7}{2K_0}\frac{L\Phi_{\text{throat}}}{2\pi R b_{\text{throat}}}\left[\frac{Q_{\text{throat}}}{\Phi_{\text{throat}}} - \alpha(H)\right]\right\} ,$$

where $H = [A(1-\delta)T_1 + (G/\Phi_{\text{throat}})T_2]$, with

$$T_1 = \frac{\lambda}{L}\left[1 - \exp(-L/\lambda)\right]\left[\varepsilon - \frac{\lambda}{L}(1-\varepsilon)\right] - \varepsilon\ \exp(-L/\lambda)$$
$$+\ (1-\varepsilon)\frac{\lambda}{L}\left[\frac{\lambda}{L}\ \exp(-L/\lambda) + \left(1 - \frac{L}{\Lambda}\right)\right]$$

and

$$T_2 = \frac{1}{2} - \frac{\lambda}{b_{\text{plate}}}(1-\varepsilon)^{-1} \exp(-b_t / L)\left\{1 - \frac{\lambda}{\delta b}\frac{1-\exp\left[-b_p(1-\varepsilon)/\lambda\right]}{1-\varepsilon}\right\} .$$

For v_{throat} we use

$$v_{\text{throat}} = c_{s,\text{throat}}\left[\frac{\Phi_{\text{plate}}}{\Phi_{\text{throat}}}\sqrt{\frac{T_{\text{plate}}}{T_{\text{throat}}}} - \sqrt{\left(\frac{\Phi_{\text{plate}}}{\Phi_{\text{throat}}}\right)^2 \frac{T_{\text{plate}}}{T_{\text{throat}}} - 1}\right] .$$

2.2 SCRAPE-OFF LAYER

The mass, momentum, and energy balance equations are used to connect the inner and outer divertor channels through the scrape-off layer. No explicit assumption is made with respect to the existence of a "watershed," or symmetry, point. Instead, the inner and outer scrape-off layer solutions are matched by requiring continuity. This approach is suggested both by the observed asymmetry in particle and energy fluxes in divertor experiments and by the plan to bias the divertor plates in the DIII-D Advanced Divertor Project to influence scrape-off layer properties.

The resulting equations are

$$\Phi_5 - \Phi_4 = \Gamma_{82} + \Gamma_{93} + \Sigma_p f_3 + \Sigma_p(1 - f_3)$$

and

$$Q_5 - Q_4 = -\alpha\,(\Gamma_{82} + \Gamma_{93}) + P_{\text{in}}/2\pi Rb \ ,$$

where Φ_4 and Q_4 are negative (counter-clockwise) for a symmetric case. These equations thus express the requirement that the total particle flux (Σ_p) and heat flux ($P_{\text{in}}/2\pi Rb$), modified for ionization of the neutral influxes Γ_{82} and Γ_{93}, must be transported in steady state.

The momentum and energy balance equations couple the inner and outer throat regions:

$$\frac{2\chi_{\parallel}}{7}\left(T_4^{7/2} - T_5^{7/2}\right) = L_3 Q_5 + L_2 Q_4 + \frac{\alpha}{2}\left(L_3\Gamma_{93} - L_2\Gamma_{82}\right) - \frac{1}{2}\frac{P_{\text{in}}}{2\pi rb}\left[L_3 f_3 - L_2(1 - f_3)\right]$$

and

$$\frac{F_4^2}{n_4} + \frac{B_{\rm pol}^2}{B_T^2}\frac{2T_4}{M} = \frac{F_5^2}{n_5} + \frac{B_{\rm pol}^2}{B_T^2}\frac{2T_5}{M} .$$

The scrape-off layer density is determined by a balance between parallel and perpendicular particle fluxes,

$$-D_\perp d^2 N_{\rm e}/dx^2 = S_{\rm plasma} + S_{\rm ioniz} - N_{\rm e}/\tau_\parallel \ ,$$

where $S_{\rm plasma}$ is the efflux from the plasma into the scrape-off layer, $S_{\rm ioniz}$ is the particle source due to neutrals from the wall or divertor impinging on the scrape-off layer, $D_\perp$ is the cross-field diffusivity, and $N_{\rm e}/\tau_\parallel$ is the parallel flow loss of scrape-off layer particles to the divertor throats. This gives the solution

$$N_{\rm sep} = (\Gamma_0 + \Sigma_0\, a_{\rm ELM}/a)\,(\tau_\parallel D_\perp)^{1/2}/D_{\rm ELM} ,$$

where $N_{\rm sep}$ is the plasma density at the separatrix (which is determined from the core solution) and $a_{\rm ELM}$ is the radius outside which ELM behavior is assumed to dominate transport ($a_{\rm ELM}$ enters because the effective density gradient at the edge depends on it).

2.3 PLASMA CORE

The plasma core model is

$$\begin{aligned} -D_{\rm core}\, d^2N_{\rm e}/dr^2 &= \Sigma_{\rm fuel} , & 0 < r < a_{\rm ELM} \\ -D_{\rm ELM}\, d^2N_{\rm e}/dr^2 &= N_{\rm e}N_0 S_{\rm ioniz} , & a_{\rm ELM} < r < a \\ V_0\, dN_0/dr &= -N_{\rm e}N_0 S_{\rm ioniz} , & a_{\rm ELM} < r < a \end{aligned}$$

where $D_{\rm ELM}$ is a time-averaged diffusion coefficient based on the ELM frequency and amplitude, N_0 is the neutral density in the core, $S_{\rm ioniz}$ is the rate coefficient for electron impact ionization ($\langle\sigma v\rangle$), V_0 is the neutral velocity in the core, and all core ionization is assumed to be localized in the ELM region.

The solution for the plasma model relates the volume-average density (hence the particle confinement time) to the separatrix density:

$$\langle N_e \rangle = N_{sep} + (\Gamma_0 V_0 / S_{ioniz} D_{ELM}) / N_{sep}$$
$$+ (a_{ELM}\, \Sigma_{fuel} / D_{core}) \{ D_{core} / D_{ELM} [1 - (a_{ELM} / a)^2] / 2 + (a_{ELM} / a)^2 / 3 \}$$

and

$$\tau_p = \langle N_e \rangle / (\Sigma_{fuel} + \Sigma_{ioniz}) \, .$$

2.4 NEUTRAL BALANCE

To form a self-consistent model the neutral balance is calculated for regions 6–9 in Fig. 1. Thus in region 6 (private flux),

$$\dot{N}_6 = 0 = \Gamma_4 \eta_{4,6} + \Gamma_5 \eta_{5,6} + \frac{1}{4}\left(1 - \eta_{9,5}\right) n_9 v_9 A_{9,5}$$
$$+ \frac{1}{4}\left(1 - \eta_{8,4}\right) n_8 v_8 A_{8,4} - \frac{1}{4} n_6 v_6 A_{6,4}$$
$$- \frac{1}{4} n_6 v_6 A_{6,5} + \frac{1}{4}\left(1 - \eta_{5,7}\right) n_7 v_7 A_{7,5} \; ;$$

in region 7 (pumping chamber),

$$\dot{N}_7 = 0 = \Gamma_5 \eta_7^{plate} + \frac{1}{4}\left(1 - \eta_{6,9}\right)\left(1 - \eta_{6,5}\right) n_6 v_6 A_{6,5}$$
$$- S n_7 \left(k T_7\right) - \frac{1}{4} n_7 v_7 A_{7,5} \; ;$$

in region 8 (inner plenum),

$$\dot{N}_8 = 0 = \Gamma_4 \eta_8^{plate} + \frac{1}{4}\left(1 - \eta_{6,4}\right) n_6 v_6 A_{6,4}$$
$$- \frac{1}{4} n_8 v_8 A_{8,4} - \frac{1}{4} n_8 v_8 A_{8,2} \; ;$$

and in region 9 (outer plenum),

$$\dot{N}_9 = 0 = \Gamma_5 \eta_9^{plate} + \frac{1}{4}\left(1 - \eta_{6,5}\right) \eta_{6,9} n_6 v_6 A_{6,5}$$
$$- \frac{1}{4} n_9 v_9 A_{9,5} - \frac{1}{4} n_9 v_9 A_{9,3} \; .$$

3. RESULTS

The pre-VORTEX model has been applied to a DIII-D divertor case to predict the range of values to be expected when divertor pumping is applied, as is proposed for the DIII-D Advanced Divertor Project. Using a data set originally compiled for DIII-D,[5] we consider the effects of applying up to 50,000 L•s of pumping to a plasma with 5 MW of injected power and 50 to 250 A of central fueling. The data required for this case are shown in Table 1.

The wall reflection coefficients R_6, R_8 and R_9 are taken as 0.98, the wall reflection coefficient in the pump region R_7 is 0.99, and the divertor reflection coefficients R_4 and R_5 are also assumed to be 0.98. The gap at the pump inlet is 3.5 cm, and room-temperature particles are assumed to be recycled there.

The plasma diffusivities D_{core} and $D_{ELM} = 5 \times 10^3$ cm^{-2}/s; $x_{ELM} = 1.0$, and $D_\perp = 5 \times 10^3$ cm^{-2}/s. The plasma efflux is assumed to be predominantly distributed to the outside ($f_3 = 0.7$).

With this reference data set, the variation of plasma core, SOL, divertor, and pump parameters is calculated for the nominal range of pumping speeds available for DIII-D: S = 0–60,000 L/s. Results for a sample case are given in Table 2. The results of the analysis for variation in pumping speed are shown in Figs. 2–5.

Figure 2(a) shows the variation in the outer divertor flux amplification factor with pumping speed. The amplification factor decreases from 10 to ~5 without significant core fueling but is maintained in the high-recycling condtion ($A \sim 10$) with core fueling of 150 to 250 A. The core density decreases by up to 50% without core

Table 1. Data required for applying pre-VORTEX

	Divertor		Scrape-off layer	
	Inner	Outer	Inner	Outer
Region (see Fig. 1)	4	5	2	3
Channel width b, cm	4.0	2.0	1.0	1.0
Poloidal length L, cm	30	40	200	260
B_T/B_{pol}	33	33	33	33
Reflection coefficient				
R (cm)	1.5	1.9	1.5	1.9
$\kappa_{\|\|}$	0.9	0.9	0.9	0.9

Table 2. Results for sample case

Power = 6.0 MW, pumping speed = 6×10^4 L/s,
average core density = 0.49×10^{20} m^{-3}, τ_p = 0.238 s

Divertor

	Outer	Inner
Region	5	4
Q, MW	4.23	–1.77
I, A	777.0	–296.0
N_{plate}, 10^{20} m^{-3}	0.45	0.01
N_{throat}, 10^{20} m^{-3}	0.81	0.01
T_{plate}, eV	37.4	366
T_{throat}, eV	41.2	366
A	7.1	1.1
Neutral pressure, torr	0.0003	0.0003
Particle flux, A		
To plate	469.4	313.9
From plate	4532.4	16.1
To private	111.8	2.0
From plenum	16.5	0.27
To scrape-off layer	777.3	296.3

Scrape-off layer

	Outer	Inner
Particle flux, A		
From plenum	81.1	0.45
From plate	7.01	0.52
Plasma efflux	689.2	295.4

Plasma core

Particle flux, A	
Fuel	40
Reflux, region 4	260.4
Reflux, region 5	28.5
Influx, region 8	225.7
Influx, region 9	330.1
Efflux, region 2	689.2
Efflux, region 3	295.4

Table 2 (continued)

Pump	
Neutral pressure, torr	0.362
Particle flux, A	
To plate	396
To private	27.7
Pumped	226.9
Back, region 5	35.3
Back, region 6	99.9
Wall pumped	61.6
Private flux	
Neutral pressure, torr	0.002
Global efficiencies	
Fraction diverted, %	6.9
Fraction trapped, %	58.4
Exhaust fraction, %	23.1

fueling [Fig. 2(b)] and is relatively constant with 150 to 130 A of core fueling. Thus, the density profile should be strongly modified by pumping.

The divertor plasma parameters are shown in Fig. 3. The plate temperature rises to ~50 eV without core fueling (as the amplification factor drops to 5) but is in the 10- to 20-eV range for core fueling rates of 150 to 250 A. Likewise, the divertor electron density can be kept at a high value (to reduce backflow of recycled neutrals) for the higher core fueling rates.

The core plasma behavior is shown in Fig. 4. The average core electron density drops significantly with pumping rates of 30,000 to 50,000 L/s with low core fueling, but can be maintained with 150 to 250 A. The particle confinement time is calculated to improve with high pumping and core fueling.

Finally, the overall exhaust efficiency of the pumping is shown in Fig. 5. The efficiency rises with an increase in pumping speed and core fueling, reaching values around 25%.

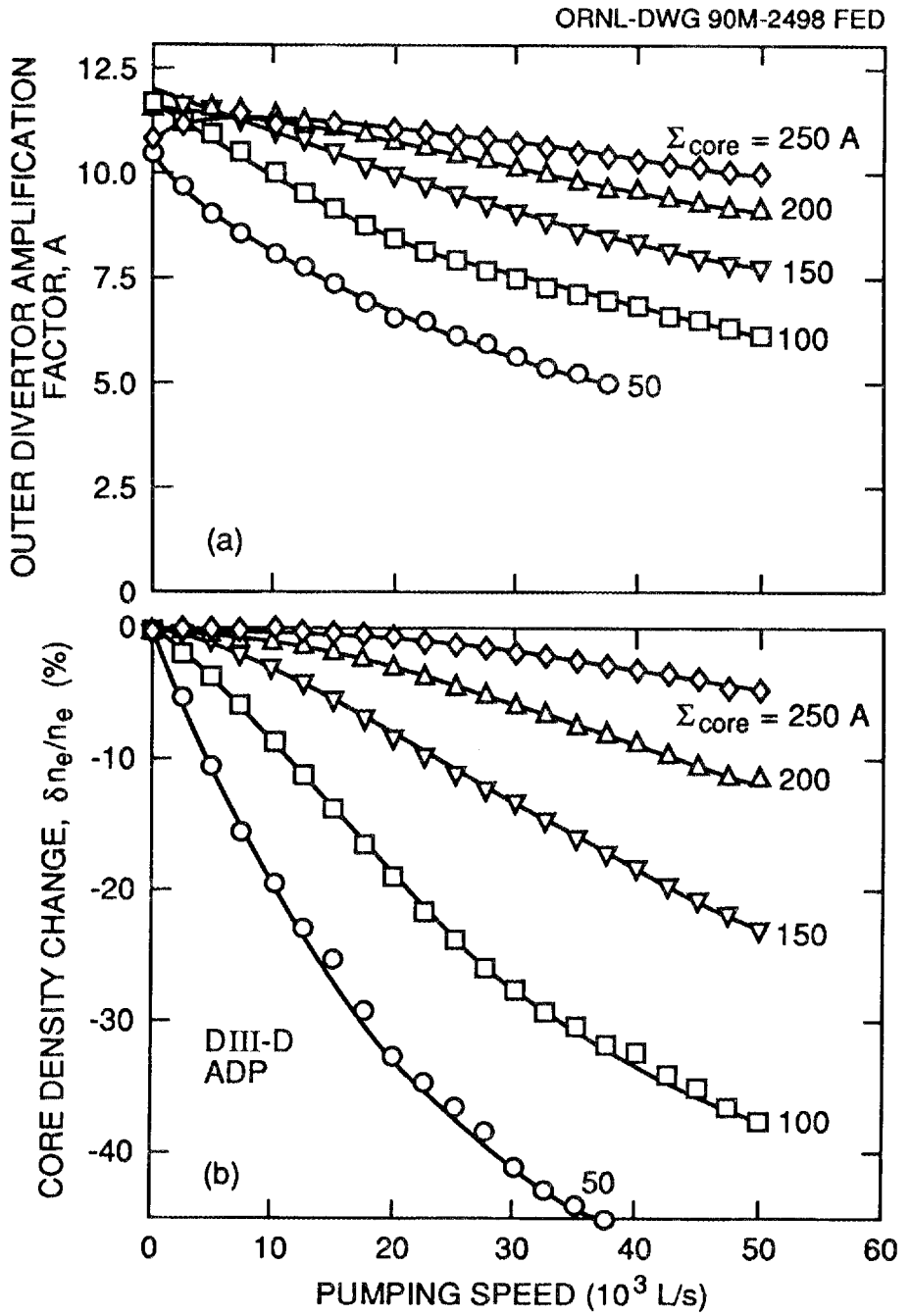

Fig. 2. (a) Variation in the outer divertor flux amplification factor with pumping speed. (b) Change in core density with pumping speed.

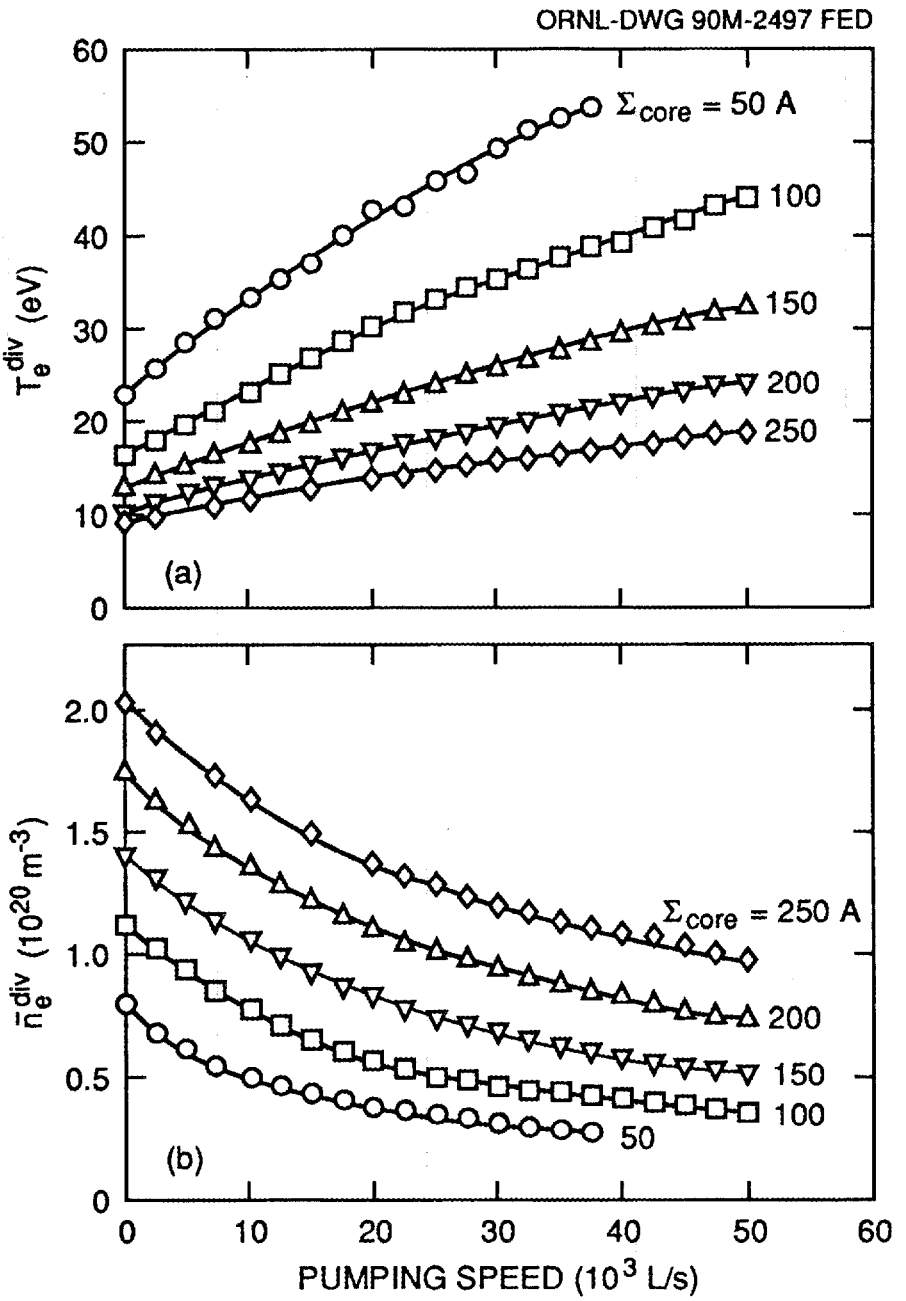

Fig. 3. (a) Temperature and (b) density of the divertor plasma as functions of pumping speed.

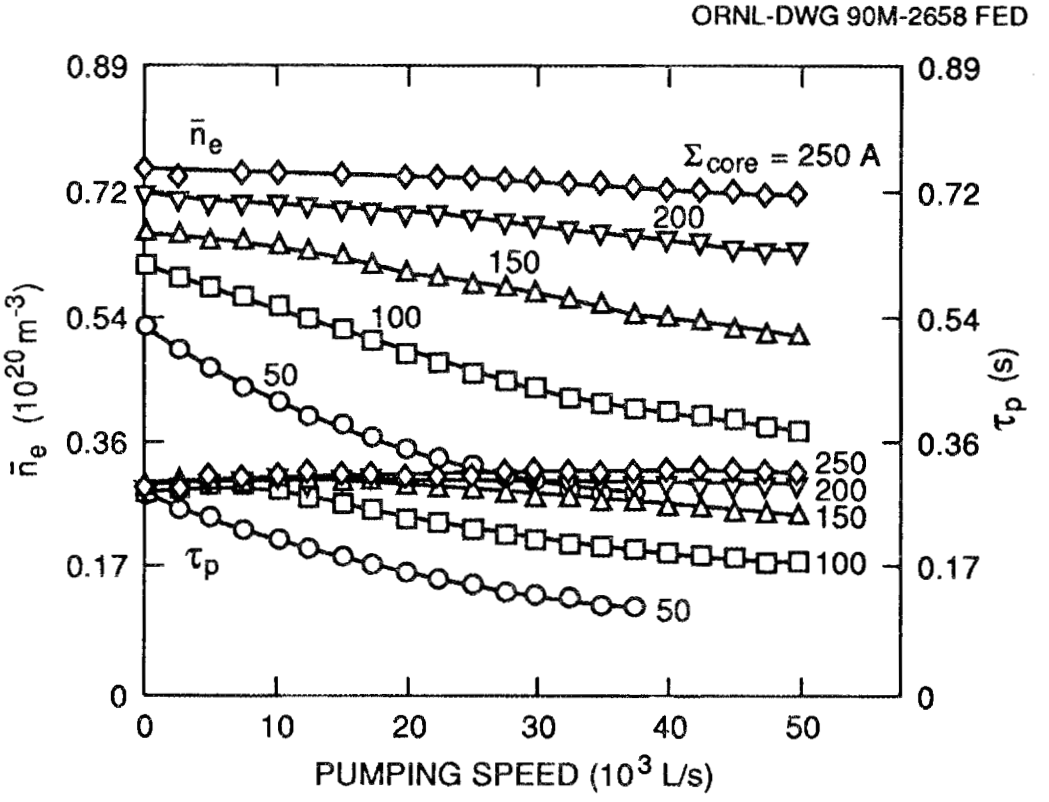

Fig. 4. Core plasma behavior.

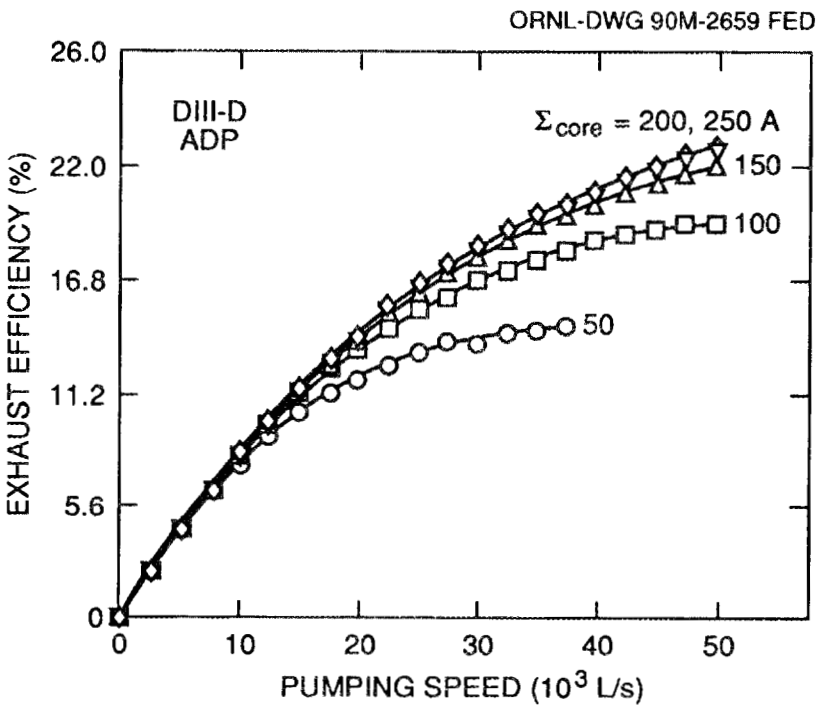

Fig. 5. Exhaust efficiency as a function of pumping speed.

REFERENCES

1. F. Wagner and K. Lackner, in *Physics of Plasma-Wall Interactions in Controlled Fusion,* ed. D. Post and R. Behrisch, Plenum, New York, 1986.

2. *ITER Conceptual Design Interim Report,* International Atomic Energy Agency, Vienna, October 1989.

3. A. Mahdavi et al., *The DIII-D Collaborative Advanced Divertor Program,* GA-A19547, General Atomics, San Diego, Calif., February 1989.

4. S. Saito et al., Nucl. Fusion **25**, 828 (1985); D. E. Post, W. Langer, and M. Petravic, J. Nucl. Mater. **121**, 171 (1984).

5. M. E. Rensink et al., "Particle Confinement Times for Divertor Discharges in DIII-D," Bull. Am. Phys. Soc. **33**, 1965 (1988).

ORNL/TM-11562
Dist. Category UC-427

INTERNAL DISTRIBUTION

1. C. C. Baker
2. L. A Berry
3. B. A. Carreras
4. R. A. Dory
5. J. L. Dunlap
6. H. H. Haselton
7–16. J. T. Hogan
17. M. S. Lubell
18. R. A. Phaneuf
19. M. J. Saltmarsh
20. J. Sheffield
21–22. Laboratory Records Department
23. Laboratory Records, ORNL-RC
24–25. Central Research Library
26. Document Reference Section
27. Fusion Energy Division Library
28–29. Engineering Technology/Fusion Energy Division Publications Office
30. ORNL Patent Office

EXTERNAL DISTRIBUTION

31. A. Pospieczszyk, Institut für Plasmaphysik, KFA Jülich GmbH, Postfach 1913, D-5170 Jülich, Federal Republic of Germany
32. Office of the Assistant Manager for Energy Research and Development, U.S. Department of Energy, Oak Ridge Operations Office, P.O. Box E, Oak Ridge, TN 37831
33. J. D. Callen, Department of Nuclear Engineering, University of Wisconsin, Madison, WI 53706-1687
34. R. W. Conn, Department of Chemical, Nuclear, and Thermal Engineering, University of California, Los Angeles, CA 90024
35. N. A. Davies, Acting Director, Office of Fusion Energy, Office of Energy Research, ER-50 Germantown, U.S. Department of Energy, Washington, DC 20545
36. S. O. Dean, Fusion Power Associates, Inc., 2 Professional Drive, Suite 248, Gaithersburg, MD 20879
37. H. K. Forsen, Bechtel Group, Inc., Research Engineering, P.O. Box 3965, San Francisco, CA 94119
38. J. R. Gilleland, L-644, Lawrence Livermore National Laboratory, P.O. Box 5511, Livermore, CA 94550
39. R. W. Gould, Department of Applied Physics, California Institute of Technology, Pasadena, CA 91125
40. R. A. Gross, Plasma Research Laboratory, Columbia University, New York, NY 10027
41. D. M. Meade, Princeton Plasma Physics Laboratory, P.O. Box 451, Princeton, NJ 08543
42. M. Roberts, International Programs, Office of Fusion Energy, Office of Energy Research, ER-52 Germantown, U.S. Department of Energy, Washington, DC 20545

43. W. M. Stacey, School of Nuclear Engineering and Health Physics, Georgia Institute of Technology, Atlanta, GA 30332
44. D. Steiner, Nuclear Engineering Department, NES Building, Tibbetts Avenue, Rensselaer Polytechnic Institute, Troy, NY 12181
45. R. Varma, Physical Research Laboratory, Navrangpura, Ahmedabad 380009, India
46. Bibliothek, Max-Planck Institut für Plasmaphysik, Boltzmannstrasse 2, D-8046 Garching, Federal Republic of Germany
47. Bibliothek, Institut für Plasmaphysik, KFA Jülich GmbH, Postfach 1913, D-5170 Jülich, Federal Republic of Germany
48. Bibliothek, KfK Karlsruhe GmbH, Postfach 3640, D-7500 Karlsruhe 1, Federal Republic of Germany
49. Bibliotheque, Centre de Recherches en Physique des Plasmas, Ecole Polytechnique Fédérale de Lausanne, 21 Avenue des Bains, CH-1007 Lausanne, Switzerland
50. R. Aymar, CEN/Cadarache, Departement de Recherches sur la Fusion Contrôlée, F-13108 Saint-Paul-lez-Durance Cedex, France
51. Bibliothèque, CEN/Cadarache, F-13108 Saint-Paul-lez-Durance Cedex, France
52. Library, Culham Laboratory, UKAEA, Abingdon, Oxfordshire, OX14 3DB, England
53. Library, JET Joint Undertaking, Abingdon, Oxfordshire OX14 3EA, England
54. Library, FOM-Instituut voor Plasmafysica, Rijnhuizen, Edisonbaan 14, 3439 MN Nieuwegein, The Netherlands
55. Library, National Institute for Fusion Science, Chikusa-ku, Nagoya 464-01, Japan
56. Library, International Centre for Theoretical Physics, P.O. Box 586, I-34100 Trieste, Italy
57. Library, Centro Richerche Energia Frascati, C.P. 65, I-00044 Frascati (Roma), Italy
58. Library, Plasma Physics Laboratory, Kyoto University, Gokasho, Uji, Kyoto 611, Japan
59. Plasma Research Laboratory, Australian National University, P.O. Box 4, Canberra, A.C.T. 2601, Australia
60. Library, Japan Atomic Energy Research Institute, Naka Fusion Research Establishment, 801-1 Mukoyama, Naka-machi, Naka-gun, Ibaraki-ken, Japan
61. G. A. Eliseev, I. V. Kurchatov Institute of Atomic Energy, P.O. Box 3402, 123182 Moscow, U.S.S.R.
62. V. A. Glukhikh, Scientific-Research Institute of Electro-Physical Apparatus, 188631 Leningrad, U.S.S.R.
63. I. Shpigel, Institute of General Physics, U.S.S.R. Academy of Sciences, Ulitsa Vavilova 38, Moscow, U.S.S.R.
64. D. D. Ryutov, Institute of Nuclear Physics, Siberian Branch of the Academy of Sciences of the U.S.S.R., Sovetskaya St. 5, 630090 Novosibirsk, U.S.S.R.
65. O. Pavlichenko, Kharkov Physical-Technical Institute, Academical St. 1, 310108 Kharkov, U.S.S.R.
66. Deputy Director, Southwestern Institute of Physics, P.O. Box 15, Leshan, Sichuan, China (PRC)
67. Director, The Institute of Plasma Physics, P.O. Box 26, Hefei, Anhui, China (PRC)

68. D. H. Crandall, Division of Applied Plasma Physics, Office of Energy Research, ER-542, Germantown, U.S. Department of Energy, Washington, DC 20545
69. D. Markevich, Division of Applied Plasma Physics, Office of Energy Research, ER-542, Germantown, U.S. Department of Energy, Washington, DC 20545
70. R. H. McKnight, Experimental Plasma Physics Research Branch, Division of Applied Plasma Physics, Office of Energy Research, ER-542, Germantown, U.S. Department of Energy, Washington, DC 20545
71. E. Oktay, Division of Confinement Systems, Office of Energy Research, ER-55, Germantown, U.S. Department of Energy, Washington, DC 20545
72. W. L. Sadowski, Fusion Theory and Computer Services Branch, Division of Applied Plasma Physics, Office of Energy Research, ER-541, Germantown, U.S. Department of Energy, Washington, DC 20545
73. R. E. Mickens, Atlanta University, Department of Physics, Atlanta, GA 30314
74. M. N. Rosenbluth, University of San Diego, La Jolla, CA 92037
75. D. Schnack, SAIC, 10260 Campus Point Drive, San Diego, CA 92121
76. Duk-In Choi, Department of Physics, Korea Advanced Institute of Science and Technology, P.O. Box 150, Chong Ryang-Ri, Seoul, Korea
77. Library of Physics Department, University of Ioannina, Ioannina, Greece
78. C. De Palo, Library, Associazione EURATOM-ENEA sulla Fusione, CP 65, I-00044 Frascati (Roma), Italy
79. Theory Department Read File, c/o D. W. Ross, Institute for Fusion Studies, University of Texas, Austin, TX 78712
80. Theory Department Read File, c/o R. Parker, Director, Plasma Fusion Center, NW 16-202, Massachusetts Institute of Technology, Cambridge, MA 02139
81. Theory Department Read File, c/o R. White, Princeton Plasma Physics Laboratory, P.O. Box 451, Princeton, NJ 08543
82. Theory Department Read File, c/o L. Kovrizhnykh, Lebedev Institute of Physics, Academy of Sciences, 53 Leninsky Prospect, 117924 Moscow, U.S.S.R.
83. Theory Department Read File, c/o B. B. Kadomtsev, I. V. Kurchatov Institute of Atomic Energy, P.O. Box 3402, 123182 Moscow, U.S.S.R.
84. Theory Department Read File, c/o T. Kamimura, National Institute for Fusion Studies, Nagoya 464, Japan
85. Theory Department Read File, c/o C. Mercier, Departemente de Recherches sur la Fusion Controlee, B.P. No. 6, F-92260 Fontenay-aux-Roses (Seine), France
86. Theory Department Read File, c/o T. E. Stringer, JET Joint Undertaking, Abingdon, Oxfordshire OX14 3EA, United Kingdom
87. Theory Department Read File, c/o R. Briscoe, Culham Laboratory, Abingdon, Oxfordshire OX14 3DB, United Kingdom
88. Theory Department Read File, c/o D. Biskamp, Max-Planck-Institut fur Plasmaphysik, Boltzmannstrasse 2, D-8046 Garching, Federal Republic of Germany
89. Theory Department Read File, c/o T. Takeda, Japan Atomic Energy Research Institute, Tokai Fusion Research Establishment, Tokai-mura, Naka-gun, Ibaraki-ken, Japan

90. Theory Department Read File, c/o J. Greene, General Atomics, P.O. Box 85608, San Diego, CA 92138-5608
91. Theory Department Read File, c/o R. Cohen, Lawrence Livermore National Laboratory, P.O. Box 5511, Livermore, CA 94550
92. Theory Department Read File, c/o R. Gerwin, CTR Division, Los Alamos National Laboratory, P.O. Box 1663, Los Alamos, NM 87545
93. D. Reiter, Institut für Plasmaphysik, KFA Jülich GmbH, Postfach 1913, D-5170 Jülich, Federal Republic of Germany
94. A. Nicolai, Institut für Plasmaphysik, KFA Jülich GmbH, Postfach 1913, D-5170 Jülich, Federal Republic of Germany
95. D. Post, Princeton Plasma Physics Laboratory, P.O. Box 451, Princeton, NJ 08543
96. W. Langer, Princeton Plasma Physics Laboratory, P.O. Box 451, Princeton, NJ 08543
97. S. Cohen, Princeton Plasma Physics Laboratory, P.O. Box 451, Princeton, NJ 08543

98–145. Given distribution as shown in OSTI-4500, Magnetic Fusion Energy (Category Distribution UC-427, Theoretical Plasma Physics)